Civil Engineering and Architecture 13(6): 4534-4545, 2025 http://www.hrpub.org
DOI: 10.13189/cea.2025.130629

Assessing the Performance of HEC-RAS 2D for Flash Flood Simulation in Mountainous Rural Eco-Tourism Area of Kampung Melangkap, Malaysia

Rosdianah Ramli[1], Janice Lynn Ayog[1,2,*], Ejria Saleh[2,3], Mohammad Radzif Taharin[1]

[1]Faculty of Engineering, Universiti Malaysia Sabah, Malaysia
[2]Natural Disaster Research Centre, Universiti Malaysia Sabah, Malaysia
[3]Borneo Marine Research Institute, Universiti Malaysia Sabah, Malaysia

Received July 29, 2025; Revised September 20, 2025; Accepted November 19, 2025

Cite This Paper in the Following Citation Styles

(a): *[1] Rosdianah Ramli, Janice Lynn Ayog, Ejria Saleh, Mohammad Radzif Taharin , "Assessing the Performance of HEC-RAS 2D for Flash Flood Simulation in Mountainous Rural Eco-Tourism Area of Kampung Melangkap, Malaysia," Civil Engineering and Architecture, Vol. 13, No. 6, pp. 4534 - 4545, 2025. DOI: 10.13189/cea.2025.130629.*

(b): *Rosdianah Ramli, Janice Lynn Ayog, Ejria Saleh, Mohammad Radzif Taharin (2025). Assessing the Performance of HEC-RAS 2D for Flash Flood Simulation in Mountainous Rural Eco-Tourism Area of Kampung Melangkap, Malaysia. Civil Engineering and Architecture, 13(6), 4534 - 4545. DOI: 10.13189/cea.2025.130629.*

Abstract Flooding presents significant risks to rural communities, particularly those dependent on eco-tourism. While HEC-RAS 2D hydrodynamic modelling is widely applied in urban and lowland areas, limited research has evaluated its performance in rural, mountainous terrains where infrastructure and flood vulnerability intersect. This study addresses that gap by assessing the suitability of HEC-RAS 2D for simulating a flash flood event in December 2022 in Kampung Melangkap, Sabah, Malaysia. The model integrated river discharge and water level data with high-resolution digital surface models (DSM) generated through drone surveys. Three governing equations available in HEC-RAS - Diffusive Wave (DW), Shallow Water Eulerian-Lagrangian Method (SW-ELM), and Shallow Water Local Inertia Approximation (SW-LIA) - were tested using two computational grid sizes (20 m and 25 m). Model validation was conducted using observed flood depths and interviews with local communities from the most affected areas. The SW-ELM model with a 25 m computational grid produced the most accurate flood depth and extent simulations, with the smallest deviation from observed data. Among the tested configurations, it also balanced accuracy and computational efficiency, making it the most suitable option for flood modelling in the study area. These findings support the use of HEC-RAS 2D as a practical tool for flood risk assessment in rural eco-tourism regions.

Keywords HEC-RAS, 2D Flood Modelling, Rural Eco-Tourism, Shallow Water Equations, Diffusive Wave

1. Introduction

Eco-tourism industry has been used as one of the strategies to help alleviate poverty of local communities in rural areas, as the preserved nature surrounding the rural areas can be utilized in attracting outsiders and tourists. In Malaysia, eco-tourism industry in the rural areas has been recognized since 1996, and the study by Abdullah et al. [1] has found that eco-tourism has provided significant economic benefits to the local community, and thus also reduce poverty in the rural areas. Therefore, the occurrence of flooding, which is the most frequent natural hazard in Malaysia, could hurt the economy of the local community in rural areas. Furthermore, damages of flooding in rural areas are more devastating compared to those in urban areas due to poverty, limited or poor infrastructures, and limited access to resources. Additionally, for rural areas involved in the eco-tourism industry, the flood impacts could be aggravated by human activities and interventions

in the natural environment [2]. Nevertheless, it is possible to reduce the impacts with adequate flood risk management strategies with information about the flooding events and possible inundation areas [2] and this can be performed with flood inundation models [3], [4].

Flood inundation modelling is used to simulate flood events, where interpretation of the flood inundation maps developed in the models enables the analysis of flood risk and damage estimation. This analysis is made for any decision-making procedure with respect to flood risk management i.e., forecasting and/or counteractive measures of flooding [5], [6], [7], [8], [9]. Generally, there are three approaches for flood inundation modelling: empirical methods, hydrodynamic modelling, and simplified conceptual modelling [7], [10]. Empirical methods are the earliest approach used for flood modelling and are majorly used in approximately 46.2% utilization in studies [11], while hydrodynamic modelling approaches are following close with 43.8% of the studies and 10% for the conceptual modelling [10]. Empirical methods are analysis of previous flood events using remote sensing detection [4] while hydrodynamic models are mathematical models that simulate the flood water movement by solving numerical equations formulated by applying laws of physics. The simplified conceptual models, as the name implies, are based on simplified hydrodynamic models with run times orders of magnitude shorter than the hydrodynamic models [7]. Amongst these approaches, Teng et al. [12] argued that the hydrodynamic modelling approach is effective in evaluating flood maps considering high spatiotemporal resolution due to its ability to include momentum and acceleration of flow in addition to continuity and mass balance.

The flood inundation maps developed from hydrodynamic modelling can give crucial spatial distribution information in terms of the flood characteristics such as flood depth and flood extent [3], [13]. For instance, flood depth showcases the severity of the flooding damage while the flood extent identifies the affected and/or vulnerable areas [14], [15]. The hydrodynamic models can be represented in one-dimensional (1D) model, two-dimensional (2D) model and three-dimensional (3D) model based on the study area and purpose of the project [2]. The most used model is the 2D model as it gives more accuracy than the 1D model and is less complex than 3D models [7], [15]. Furthermore, the development of more reliable numerical methods, efficient computing power and innovative topographic survey techniques enhanced the widespread use of the 2D hydrodynamic models [16], [17]. One of the most widely used software for 2D flood modelling is the Hydrologic Engineering Center – River Analysis System (HEC-RAS) software [18].

The HEC-RAS software was developed by the United States Army Corps of Engineers (USACE) in 1995 and has been continuously improved to the point that it is widely used in the scientific and technical fields [19], [20]. For example, HEC-RAS software has been developed from 1D modelling to mixed 1D-2D modelling and full 2D modelling. Such improvement has allowed HEC-RAS to have a wide range of applications and be able to deploy different schematization complexities [2], [21] especially for 2D modelling. However, it was also reported that HEC-RAS might not be adaptable to represent extended period simulations [22]. Nevertheless, the efficiency of HEC-RAS for 2D flood modelling in developing flood inundation maps has been proven in countless studies such as [3], [8], [17], [23], [24], [25], [26]. The HEC-RAS 2D model capabilities are also well established in benchmarking testing against other industrial flood modelling packages [27]. USACE itself has adopted benchmarking tests conducted by the United Kingdom Environment Agency for HEC-RAS version 5.0 [19].

In 2016, Paudel et al. [28] presented their study in comparing HEC-RAS 2D modelling with TUFLOW and MIKE21 models where they found that HEC-RAS results were consistent with the other flood modelling packages. Almost a decade after that, another study by Artiglieri et al. [29] also compared HEC-RAS with TUFLOW, this time with a newer version, and found that HEC-RAS is on par with TUFLOW at higher grid resolution. On the other hand, Shrestha et al. [4] made a benchmarking study for HEC-RAS and MIKE21 for flooding in an urban area. While they found that both software packages were suitable to depict the time series result for a given flow condition, it was also found that visualization feature in HEC-RAS has helped to provide a clear understanding of the flooding event. Recently, Bragg et al. [22] conducted a benchmarking study comparing HEC-RAS version 6.3 with SWMM models in a semi-urbanized watershed where the HEC-RAS results were comparable to the SWMM models under certain conditions.

As mentioned earlier, HEC-RAS itself has been improved from time to time. For instance, the HEC-RAS software has incorporated additional governing equations of the shallow water equations, implemented through numerical solution approaches, to enhance its 2D modelling. In version 5, the HEC-RAS 2D model employs Shallow Water equations (SW) (also known as Saint-Venant equations) and Diffusive Wave equations (DW) [16], [24]. The SW equations use Eulerian-Lagrangian method (SW-ELM) that employs full momentum equations while DW is the simplification of SW where the inertial terms were neglected [27], [30]. Another approach to SW equations was added in version 6.1 which uses Eulerian method (SW-EM) and in version 6.3, a third approach i.e., the local inertia approximation (SW-LIA) was added. Due to its stronger momentum conservation, SW-EM typically demands longer simulation times than other governing equations and may also exhibit stability challenges [31]. SW-LIA is a simplification of SW-ELM, but unlike DW, SW-LIA neglects the acceleration terms but keeps the

inertial terms intact. However, SW-LIA is notably faster and more stable, in addition to being able to produce comparable results to the other governing equations for a range of flood modelling applications. Previous investigations into both SW-ELM and SW-LIA - for example, [32], [33], [34] - together with other studies demonstrating the efficiency of the local inertia approximation in modelling gradually varied flows and high-resolution terrains [35], [36], [37], [38], provide broader evidence of the method's potential advantages across diverse modelling contexts.

While HEC-RAS 2D modelling has been benchmarked across various flood scenarios, previous studies have largely focused on urban settings or conventional hydrological contexts. To date, no benchmarking has assessed the use of HEC-RAS 2D in mountainous rural eco-tourism landscapes that are frequently affected by flooding, where such events pose significant challenges for effective evacuation strategies and long-term resilience planning. This study addresses that gap by evaluating the model's suitability in such a complex setting, where hydrological dynamics and land-use sensitivities differ markedly. The analysis is based on a single, documented flood event that occurred in December 2022 in Kampung Melangkap - the first verified flood with sufficient hydrological and topographical data, confirmed by local community accounts, and occurring in the context of rapid eco-tourism expansion after the year 2020, following the COVID-19 pandemic.

2. Materials and Methods

A mountainous rural eco-tourism area in Sabah, Malaysia, was chosen for this study as its eco-tourism activities were severely affected by a recent flood event. The study area, Kampung Melangkap in Kota Belud district, was chosen due to its unique history of debris flow, the sudden expansion of eco-tourism activities after the year 2020, and the occurrence of its first recorded flood. Further elaboration on the study area is discussed in the next section (Sec. 2.1).

For this study, 2D flood models were developed using HEC-RAS software version 6.5. The overall modelling framework is outlined in the methodological flowchart in Figure 1. HEC-RAS 2D requires both hydrological and topographical input data; accordingly, river water depth and discharge measurements were compiled for the study area, while topographical data were derived from a Digital Surface Model (DSM). Model simulations were carried out using three selected sets of numerical governing equations available within HEC-RAS. For consistency, the same computational mesh, time step, and simulation duration were applied across all models, so that the differences in performance reflect the inherent behavior of the equations rather than optimization choices.

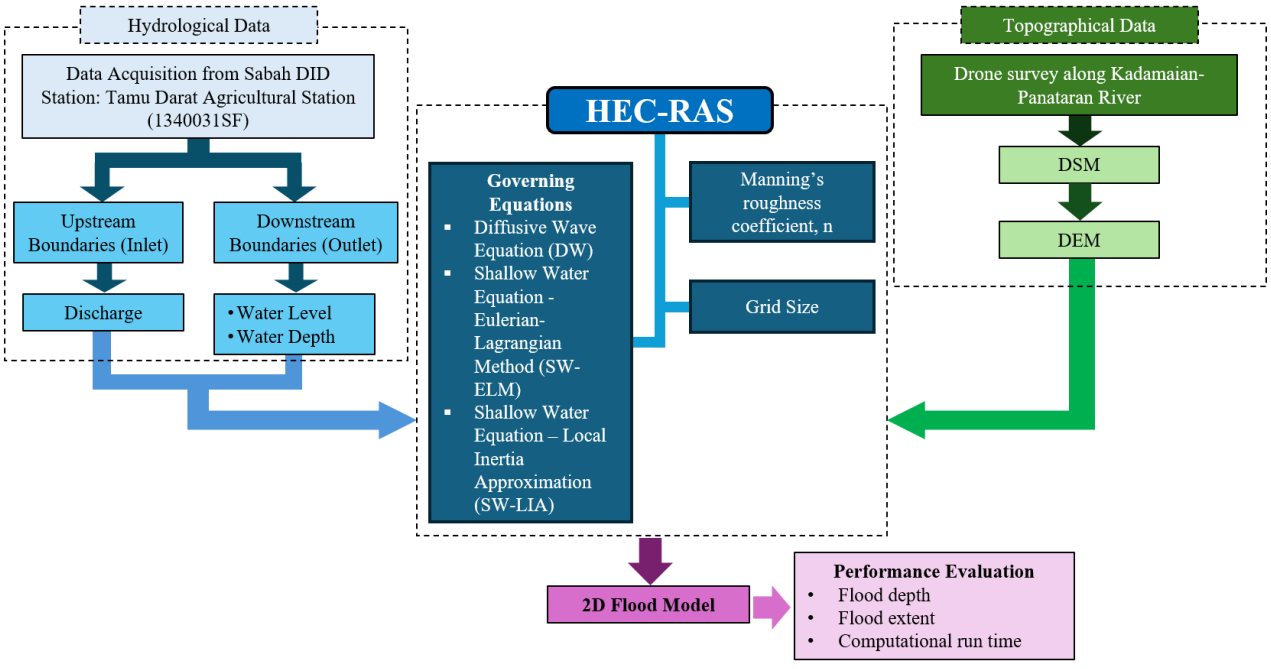

Figure 1. Methodology flowchart for HEC-RAS 2D modelling

2.1. Background of Study Area

The study area (Figure 2) is in Kota Belud district, Sabah, Malaysia, approximately 76 km from the state capital, Kota Kinabalu. There are three major catchment areas in Kota Belud, namely Tempasuk catchment, Wariu catchment, and Kadamaian catchment [39]. The study area is situated in the Kadamaian catchment area (359.36 km^2), where it covers the downstream section of Kadamaian river i.e. from the Tamu Darat Agricultural Station at the downstream (inset of Figure 2, brown line) to the middle section of Kadamaian river (inset of Figure 2, blue line), with a confluence upstream that links to a tributary river called Panataran river. The study area also covers the downstream part of Panataran river i.e. from the confluence to the bailey bridge situated within the village of Melangkap (inset of Figure 2, black line). The total length of the river of interest, herein mentioned as the Kadamaian-Panataran river in this paper, is approximately 15 km with a mean slope of 3.2%. The river originates from Mount Kinabalu [40] and the main source of flow is the runoffs on the surfaces of Mount Kinabalu.

About 12 km from the foothill of Mount Kinabalu is the village of Melangkap (or "Kampung Melangkap" as known locally), which is situated along the Panataran river. The local communities in Kampung Melangkap established eco-tourism premises along the Panataran River such as homestays and camping sites in May 2019 [41], [42] after they were severely affected by a post-seismic debris flow event which expanded the Panataran river corridor and shallowed the riverbed [43], [44]. The braiding process of the Panataran river inadvertently improved the river aesthetics with more sand bars formation that revealed along the river channel.

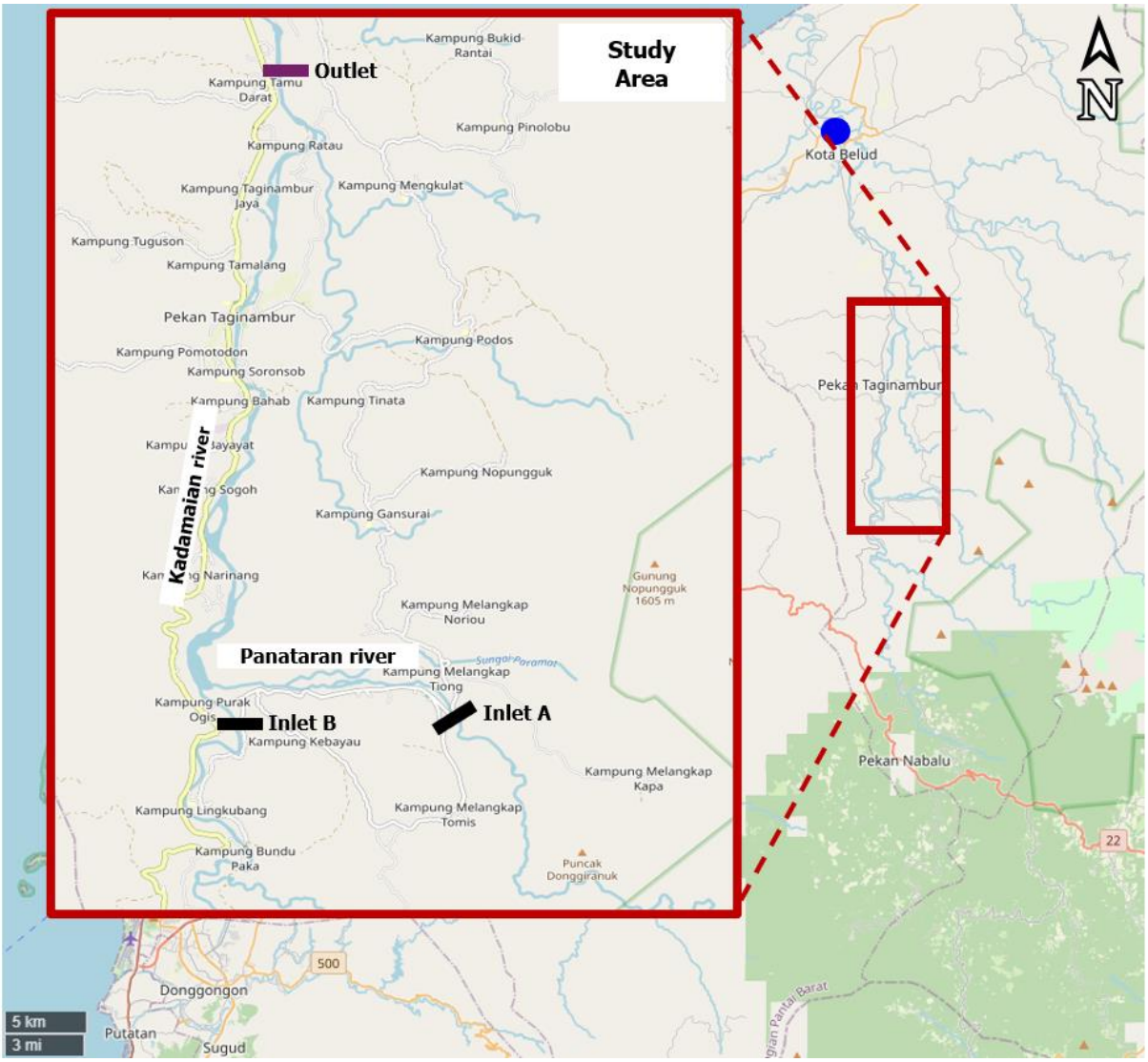

Figure 2. Location of the study area (red box) in Kota Belud, Sabah, Malaysia. The inset shows the zoomed-in image of Kadamaian-Panataran river with inlets and outlets set for the HEC-RAS 2D model. The first inlet (Inlet A) is marked with black line at the Panataran river's bailey bridge, while the second inlet (Inlet B) is marked with black line at the middle section of Kadamaian river right before the Kadamaian-Panataran confluence. The outlet, marked with a brown line is at the downstream of Kadamaian river, specifically at the Tamu Darat Agricultural Station

The climate in the area is equatorial with mean annual rainfall of 2547.2 mm and high temperatures between 32.2 ℃ and 44.3 ℃ [40]. The Northeast monsoon with strong winds (November – March) and Southwest monsoon with lower humidity (late May – September) not only influenced the area but also brought heavy rainfall and increased river flow discharges. Exposure to both monsoon seasons, together with changes in braiding [45] in the Panataran river made Kampung Melangkap susceptible to flash floods from Panataran river whenever there is heavy rainfall at Mount Kinabalu. For example, from the 21st to 26th December 2022, heavy rainfall occurred almost non-stop, eventually causing a flash flood event to occur on 25th December 2022 in Kampung Melangkap. This flood event also inundated surrounding eco-tourism areas, trapping 25 visiting tourists at one of its camping sites [46].

2.2. Collation of Hydrological and Topographical Data

Hydrological data available in the year 2022 were obtained from the Sabah State Department of Irrigation and Drainage. This year was chosen to capture the most recent flash flood event that occurred from 21st to 26th December 2022 in Kampung Melangkap. The hydrological data obtained were daily water level and river discharge, taken from Tamu Darat Agricultural Station (Station ID: 1340031SF) records.

Figure 3 shows the Kadamaian catchment area and the rivers and sub-catchment areas. There are two inlets serving as the upstream boundaries and one outlet serving as the downstream boundary of the study domain, respectively. The discharge at the first inlet (i.e. Inlet A), located at the Panataran river's bailey bridge, is contributed by the Panataran sub-catchment with an area of 95.90 km^2 (yellow area in Figure 3) while the discharge at the second inlet (i.e. Inlet B) is contributed from the Upper Kadamaian sub- catchment with an area of 155.18 km^2 (red area in Figure 3). For each upstream boundary, the river discharge (Figure 4) was rescaled from the observed river discharge at Tamu Darat gauging station based on its catchment area. The peak discharge at Inlet A is 21.45 m^3/s and at Inlet B is 36.79 m^3/s, both on 22nd December 2022. The outlet is downstream of Kadamaian river, where Tamu Darat Agricultural Station is situated. Water depths were calculated from observed water levels, referenced to an estimated datum corresponding to the lowest recorded discharge in December 2022, as documented by the gauging station. The highest water depth within the one-week period is 1.42m on 23rd December 2022 as shown in Figure 4.

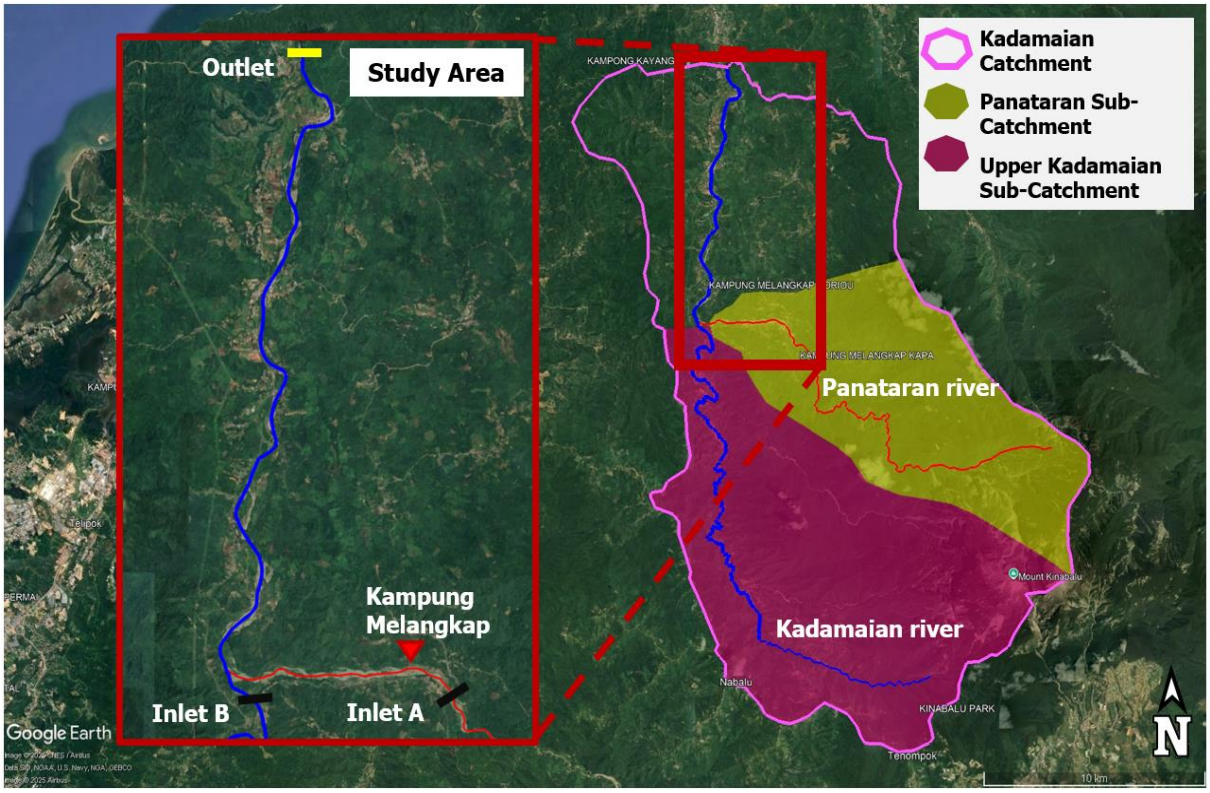

Figure 3. Satellite image from Google Earth Pro showing the Kadamaian catchment area and sub-catchment areas related to the study area

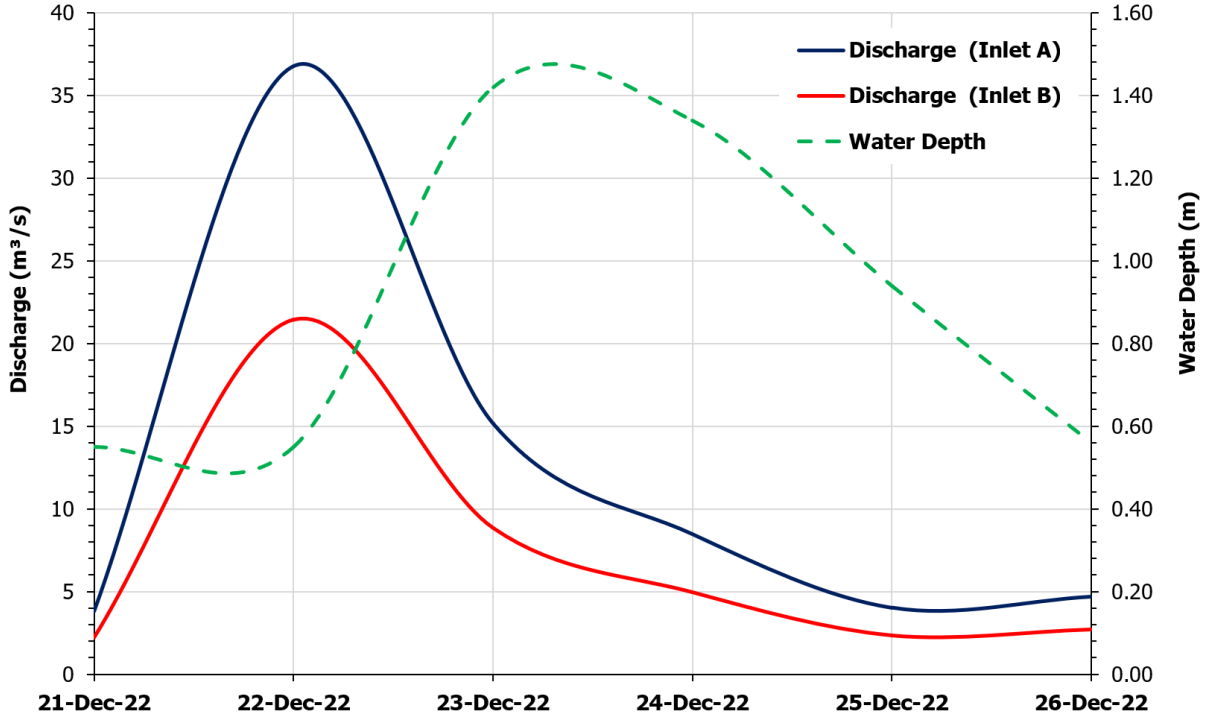

Figure 4. River discharges data for upstream boundaries (i.e. Inlet A and Inlet B), and river water depth for downstream boundary at Tamu Darat Agricultural Station for 21st to 26th December 2022

In addition to the hydrological data, topographical data, which are the terrain model of Kampung Melangkap and Kadamaian-Panataran river, were also collated. For this purpose, a drone survey was carried out along the Kadamaian-Panataran river. The drone used for this work was DJI Phantom, flown at the height of 200 m above the ground surface. The output from the drone was processed using Agisoft Metashape Professional version 2.1.1 software package, where the digital surface model (DSM) for the study area was created. A grid resolution of 35 cm × 35 cm was chosen as optimal for the generated DSM, providing sufficient detail to capture terrain features while remaining computationally manageable for HEC-RAS modelling.

To calibrate and verify the HEC-RAS 2D model, a site visit was made to the Panataran river and Kampung Melangkap on 4th December 2024 to obtain information on December 2022 flood event. Interviews with the local communities were conducted in which information on locations affected by the flood and estimated flood depth at those locations were provided. Based on the responses, three key locations were identified (Figure 5) and the flood water depth in those locations was recorded (Table 1). These identified locations, of which two (i.e. Location 2 and Location 3) are popularly community-run eco-tourism premises in Kampung Melangkap, were the worst affected locations during the December 2022 flood event.

2.3. Flood Modelling Using HEC-RAS

The flood model was developed using hydrological and topographical data as outlined in Sec. 2.2. Topographical inputs, derived from a drone-based DSM survey, were integrated into HEC-RAS via the RAS Mapper tool to define the terrain. A sensitivity analysis was conducted, resulting in the selection of 0.05 as the Manning's roughness coefficient (n) for use in this study. Two computational grids, namely 20 m × 20 m (24,566 cells) and 25 m × 25 m (15,655 cells), were configured for model evaluation, and the optimal grid will be identified based on performance across all three governing equations.

As explained earlier in Sec. 1, HEC-RAS includes four governing equations of the shallow water equations, implemented through numerical solution approaches, for 2D flow modelling: DW, SW-ELM, SW-EM and SW-LIA. However, due to the high computational cost and instability associated with the SW-EM approach, especially when applied to complex terrain [27] such as that used in this study, it has been excluded from the modelling approach. Accordingly, the flood models developed utilize three approaches i.e. DW, SW-ELM, and SW-LIA, which will collectively be referred to as 'flood models' throughout this paper.

For the sake of brevity, detailed explanations of the numerical schemes are not provided herein; readers are referred to the HEC-RAS reference manual for further information.

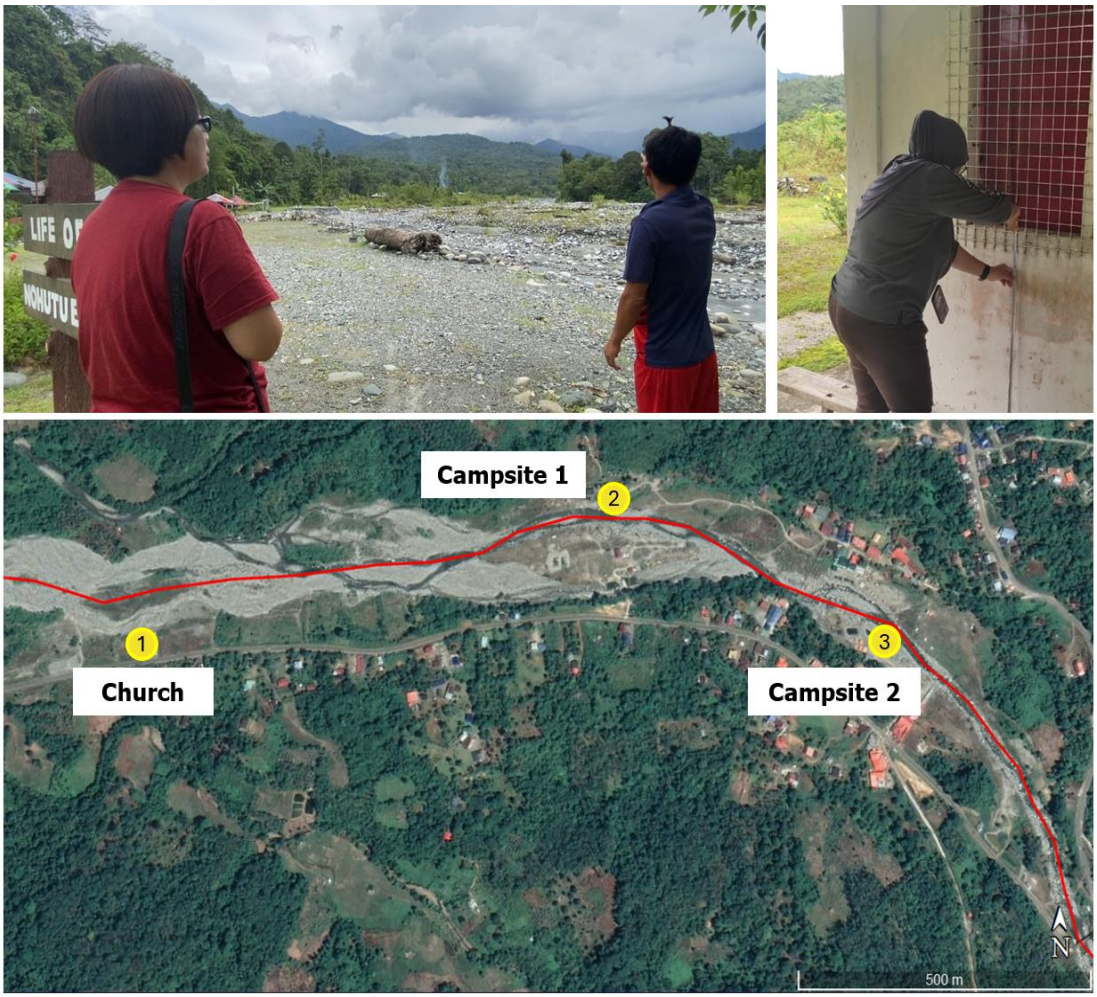

Figure 5. Site visit at Kadamaian-Panataran river and surrounding area where interviews with locals were conducted (top left panel) and the observed flood depth was measured (top right panel); and the affected locations identified from the site visit (bottom panel)

Table 1. Information on identified location along Panataran river

Location ID	Location	Coordinate	Ground level (m)	Observed flood depth (m)
1	Old Village Church (in Datau)	6 °9'59.49"N, 116 °28'6.83"E	145.21	1.2
2	Campsite 1 (near Nohutu)	6 °10'7.14"N, 116 °28'33.08"E	160.00	1.2
3	Campsite 2 (near Polumpong)	6 °10'0.78"N, 116 °28'46.01"E	171.27	1.3

3. Results and Discussions

In this section, the assessments of the flood models' performance are discussed based on flood depth, flood extent, and the computational runtime. The flood depth assessment evaluates the suitability of HEC-RAS 2D model in simulating flooding in Panataran river and Kampung Melangkap, while the flood extent assessment highlights the extent and severity of flooding that occurred in the study area in December 2022 flood event. Finally, the computational runtime of each flood model configuration was evaluated, with performance benchmarks guiding the selection of the most efficient and stable 2D scheme suitable for simulating flood dynamics within the study area.

3.1. Flood Depth

The first performance assessment for the flood models is flood depth at the three identified locations, where the simulated flood depths in HEC-RAS are compared to the observed flood depths during the December 2022 flood event. Figure 6 shows the simulated flood depths for all three locations using different computational grids. To support model evaluation, the percentage difference between simulated and observed flood depths is also presented in Figure 6.

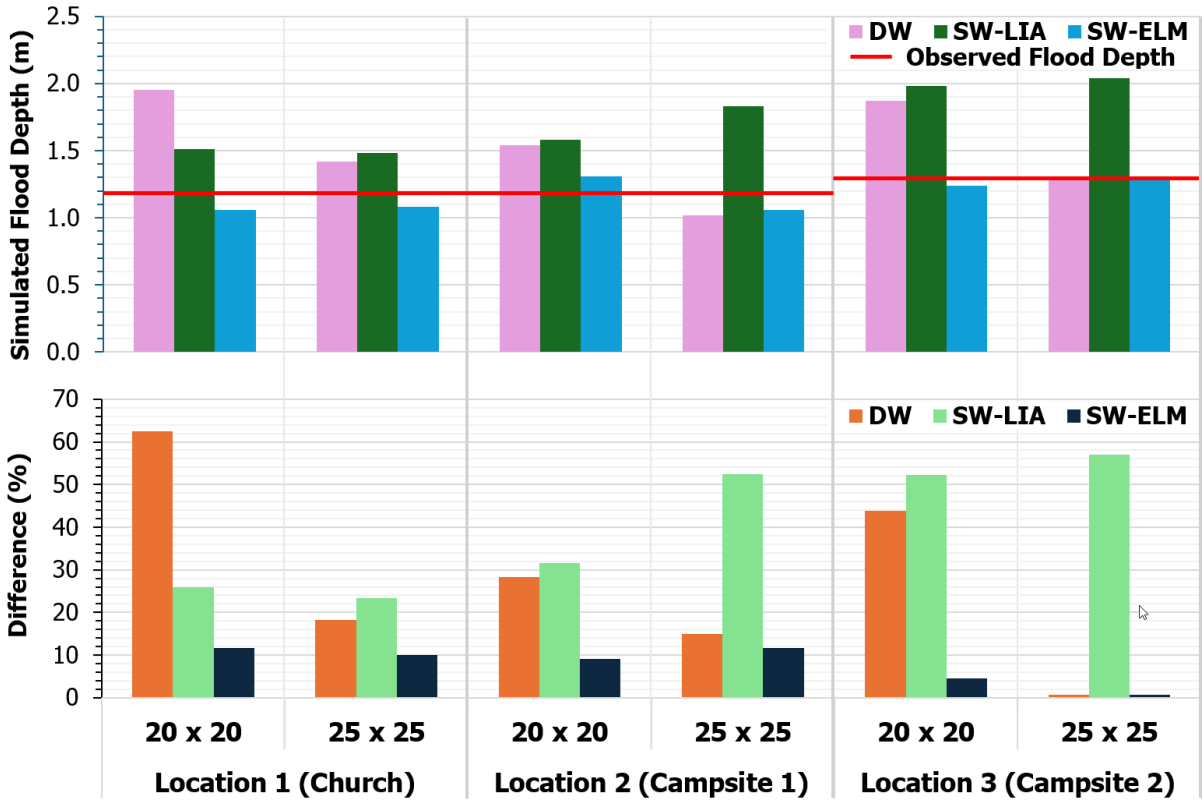

Figure 6. Flood depths at three locations in the study area simulated by HEC-RAS 2D models with different computational grids, in comparison to the observed flood depth where the observed flood depth at Location 1 and 2 is 1.2m and at Location 3 is 1.3m (top panel), and percentage difference of simulated flood depth with the observed flood depth at different computational grids (bottom panel)

Overall, the simulation results show that SW-ELM model gives the best prediction for both 20 m × 20 m and 25 m × 25 m computation grids at all three locations. The simulated flood depths by SW-ELM models were mostly under-predicted, with a consistent difference of less than 12%. The most over-predicted depth was made by DW model at Location 1 (Church) using 20 m × 20 m grid size. The closest predictions were by DW and SW-ELM models at Location 3 (Campsite 2) using 25 m × 25 m grid size. Both models give a 0.8% difference, although DW model under-predicted while SW-ELM model over-predicted the simulated flood depth values.

At Location 1 (Church), SW-ELM model gives the best results for both computational grids. Although it might look like SW-ELM models under-predicted the results compared to the other two models, it has the least difference around 10% – 12%. The second-best result differs in each grid size. SW-LIA model gives the second-best result using the 20 m × 20 m grid, while DW model is the second-best using the 25 m × 25 m grid. However, DW model over-predicted the depths in lower grid spacing (62.5% difference) while SW-LIA model is slightly more consistent at both grid sizes with differences at around 23% to 25%.

At Location 2 (Campsite 1), both DW and SW-ELM models showed similar patterns where both models were over-predicting in the smaller grid spacing (20 m × 20 m) while under-predict in the bigger grid spacing (25 m × 25 m). However, SW-ELM model still gives the best prediction with the least difference for both computational grids. In comparison, SW-LIA model gives the most over-predictions at both computational grids in this location where the differences were 32% and 53% for 20 m × 20 m and 25 m × 25 m grids, respectively.

SW-ELM model showed the best prediction at Location 3 (Campsite 2) where the difference between simulated and observed flood depth was the smallest at 5% for 20 m × 20 m grid and 0.8% for 25 m × 25 m grid size. DW model gives the same close prediction for the 25 m × 25 m grid size but over-predicted in the 20 m × 20 m grid size. Nevertheless, the worst prediction was made by SW-LIA model with difference over 50% for both grid sizes.

In conclusion, the findings show that the suitable computational grid for the study area is 25 m × 25 m with the most reliable (or closest) prediction made by the SW-ELM model. This shows that HEC-RAS 2D model using SW-ELM governing equation is appropriate for the study area.

3.2. Flood Extent

Based on the findings from the flood depth assessment in Section 3.1, the 25 m × 25 m computational grid was selected to simulate flood extents for assessing the models' performance. Figure 7 shows the maximum flood extent

predicted by all models, focusing on the key locations. The flood extents produced by all three models are similar in most places along the river in the study area. However, further analysis by overlapping the flood extents' outlines as presented in Figure 7(d) shows that there are discrepancies at certain points along the river. For instance, within 1000 m east of Location 1, around Location 2, and along the bank opposite Location 3 near the upstream reach, the DW model estimated a greater flood extent than the SW-ELM model. Although the flood extent predicted by the SW-LIA model generally aligns with that of SW-ELM, slight overestimation is observed along the southern bank (approximately 500 m to 1000 m east of Location 1). Additionally, SW-LIA notably overestimates flood extent in the upstream area.

As SW-ELM model made the closest simulated flood depths in the previous analysis in comparison to the observed values, it can be said that the flood extent simulated by the SW-ELM model is the extent of flood in the December 2022 event. From the flood extent presented in Figure 7(c), the flooding has indeed affected the areas in Kampung Melangkap as well as extending all the way downstream to Location 1 (Church). The flooding occurring in the area was severe enough where the flood from the Panataran river spilled and covered the banks along the river. At Location 2 (Campsite 1) and Location 3 (Campsite 2), the areas were entirely submerged, consistent with the report by [46] in Sec. 2.1.

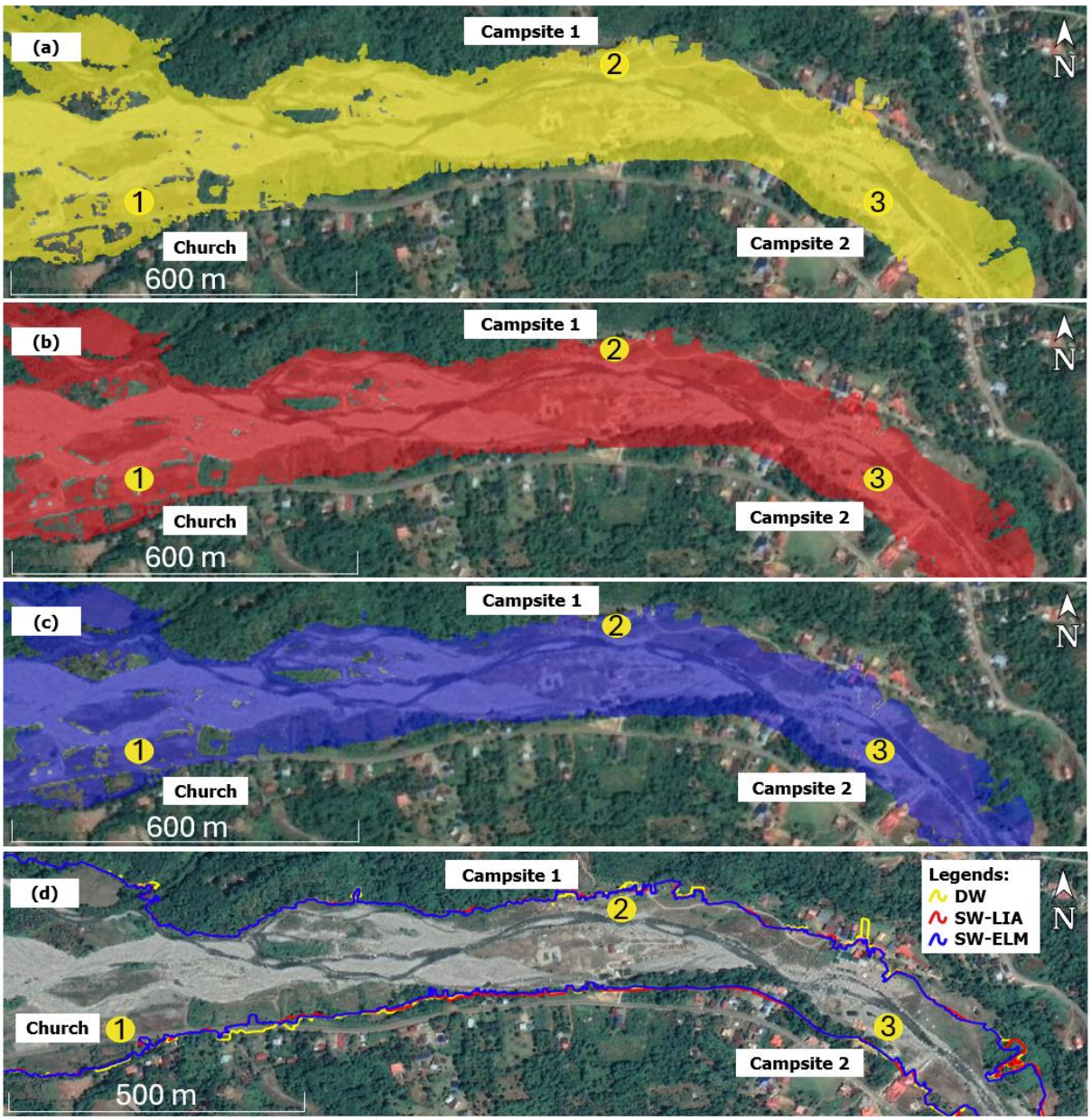

Figure 7. Flood extent in the study area using (a) diffusive wave (DW), (b) shallow water – Local Inertia Approximation (SW-LIA), (c) shallow water - Eulerian-Lagrangian Method (SW-ELM) equations, respectively, and (d) the outlines of maximum flood extent simulated by all three governing equations

3.3. Computational Runtime

The final assessment for the HEC-RAS 2D models is the computational runtime of each model. Table 2 and Figure 8 below show the runtime taken for simulations for all three models. It shows that DW models have the fastest computational runtime but as discussed earlier in Secs. 3.1 and 3.2, DW model mostly overpredicted the flood event (in terms of flood depth and flood extent). SW-LIA and SW-ELM models had competitive runtime where the computational runs for both models at different computational grids were similar, with SW-LIA being the faster one. Based on its performance in estimating flood depth and extent, the SW-ELM model is the most suitable choice for the study area, providing the closest match to observed conditions. Accordingly, employing the SW-ELM governing equation is deemed the most appropriate choice for the 2D flood model in this study area.

Table 2. Computational Runtime for different governing equations using different computational grids

Flood Model (Governing Equation)	Runtime (seconds)	
	20 × 20	25 × 25
DW	458s	309s
SW-LIA	1477s	958s
SW-ELM	1535s	972s

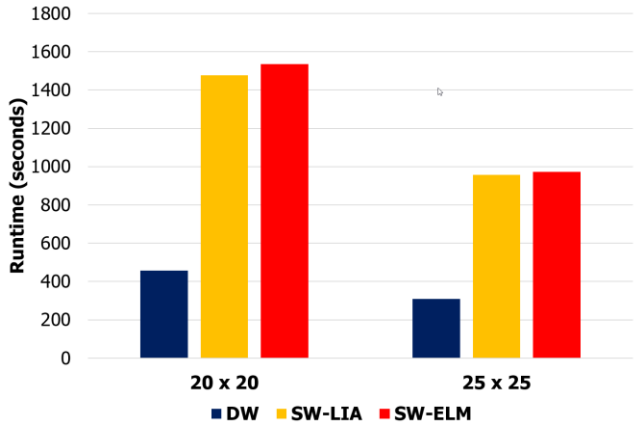

Figure 8. The computational runtimes

While SW-LIA was marginally faster in most grid configurations, under the specific conditions of a real-world, data-scarce flood in Kampung Melangkap, characterized by steep slopes, coarse and unstable sediment deposits from post-seismic debris flows, and active human use through eco-tourism facilities along the floodplain, SW-ELM was unexpectedly more computationally efficient. This outcome contrasts with earlier work on both SW-ELM and SW-LIA (e.g. [32], [33], [34]). These results indicate that the governing equations and numerical solvers used are highly site-dependent and should be validated empirically under the specific physical and data constraints of each application.

4. Conclusions

The assessments presented in this study affirm that the HEC-RAS 2D model is effective for simulating flood behavior across the complex terrain of Kampung Melangkap, Kota Belud, Sabah, an area characterized by eco-tourism activities and environmental sensitivity. Among the governing equations (implemented through numerical solution approaches) of the shallow water equations evaluated, SW-ELM not only produced the most accurate representation of flood extent and severity, but also demonstrated computational efficiency, making it the optimal choice for this case study. Its integration within the HEC-RAS framework offers reliable and timely support for localized flood risk analysis and mitigation planning.

The findings are constrained by the single-event scope of the analysis, which focused on the December 2022 flood in Kampung Melangkap - the first verified flood with sufficient hydrological and topographical data, occurring in the context of rapid eco-tourism expansion after 2020. While this focus enabled a detailed comparative assessment under real-world conditions, it may not capture variability across seasons or under different rainfall characteristics, or under varying antecedent moisture conditions. Future research should incorporate multiple flood events across varying hydrological conditions - including rainfall variability and historical moisture states - and apply this comparative framework to other mountainous rural eco-tourism areas with different topographic and hydrological profiles to strengthen the applicability of the findings. With richer datasets, further work could also examine optimization of each modelling approach to balance accuracy and efficiency.

Acknowledgements

This study is financially supported by the Universiti Malaysia Sabah Research Cluster Fund No. DKP0039. We extend our sincere appreciation to Kenneth Chung for providing aerial imagery and conducting the drone survey, along with digital surface model (DSM) processing, and to Prof. Dr. Felix Tongkul for his expert advice. We also thank the reviewers for their appropriate and constructive suggestions to improve this manuscript.

REFERENCES

[1] M. Abdullah, M. P. Mamat, N. Adnan, F. N. Tuan Hussain, "Ecotourism as Tool for Eradicating Rural Poverty in Peninsular Malaysia," IOP Conference Series: Earth and Environmental Science, Vol. 549, p. 012091, 2020. DOI: 10.1088/1755-1315/549/1/012091.

[2] N. Ongdas, F. Akiyanova, Y. Karakulov, A. Muratbayeva, N. Zinabdin, "Application of HEC-RAS (2D) for Flood

Hazard Maps Generation for Yesil (Ishim) River in Kazakhstan," Water, Vol. 12, No. 10, pp. 1–20, 2020. DOI: 10.3390/w12102672.

[3] V. A. Rangari, N. V. Umamahesh, C. M. Bhatt, "Assessment of inundation risk in urban floods using HEC RAS 2D," Modeling Earth Systems and Environment, Vol. 5, No. 4, pp. 1839–1851, 2019. DOI: 10.1007/s40808-019-00641-8.

[4] A. Shrestha, L. Bhattacharjee, S. Baral, B. Thakur, N. Joshi, A. Kalra, R. Gupta, "Understanding Suitability of MIKE 21 and HEC-RAS for 2D Floodplain Modeling," World Environmental and Water Resources Congress 2020, pp. 237–253, 2020. DOI: 10.1061/9780784482971.024

[5] A. A. M. AL-Hussein, S. Khan, K. Ncibi, N. Hamdi, Y. Hamed, "Flood Analysis Using HEC-RAS and HEC-HMS: A Case Study of Khazir River (Middle East – Northern Iraq)," Water, Vol. 14, No. 22, pp. 1-19, 2022. DOI: 10.3390/w14223779.

[6] P. Mani, C. Chatterjee, R. Kumar, "Flood hazard assessment with multiparameter approach derived from coupled 1D and 2D hydrodynamic flow model," Natural Hazards, Vol. 70, No. 2, pp. 1553–1574, 2014. DOI: 10.1007/s11069-013-0891-8.

[7] J. Teng, A. J. Jakeman, J. Vaze, B. F. W. Croke, D. Dutta, S. Kim, "Flood inundation modelling: A review of methods, recent advances and uncertainty analysis," Environmental Modelling and Software, Vol. 90, pp. 201-216, 2017. DOI: 10.1016/j.envsoft.2017.01.006.

[8] A. K. I. Pathan, P. G. Agnihotri, "2-D Unsteady Flow Modelling and Inundation Mapping for Lower Region of Purna Basin Using HEC-RAS," Nature Environment and Pollution Technology, Vol. 19, No. 1, pp. 277–285, 2020.

[9] D. Y. S. Mah, J. L. Ayog, A. H. M. Salehe, "Dual-system concept for stormwater control in commercial centre," International Journal of Advanced Technology and Engineering Exploration, Vol. 9, No. 86, 2022, DOI: 10.19101/IJATEE.2021.874685.

[10] A. Khouz, J. Trindade, P.P. Santos, S.C. Oliveira, F. El Bchari, B. Bougadir, R.A. Garcia, E. Reis, M. Jadoud, T. Saouabe, S. Rachidi, "Flood Susceptibility Assessment through Statistical Models and HEC-RAS Analysis for Sustainable Management in Essaouira Province, Morocco," Geosciences, Vol. 13, No. 12, p. 382, 2023, DOI: 10.3390/geosciences13120382.

[11] R. B. Mudashiru, N. Sabtu, I. Abustan, W. Balogun, "Flood hazard mapping methods: A review," Natural Hazards, Vol. 112, No. 3, pp. 1903-1939, 2021. DOI: 10.1016/j.jhydrol.2021.126846.

[12] J. Teng, J. Vaze, D. Dutta, S. Marvanek, "Rapid Inundation Modelling in Large Floodplains Using LiDAR DEM," Water Resources Management, Vol. 29, No. 8, pp. 2619–2636, 2015, DOI: 10.1007/s11269-015-0960-8.

[13] B. Kim, B. F. Sanders, J. E. Schubert, J. S. Famiglietti, "Mesh type tradeoffs in 2D hydrodynamic modeling of flooding with a Godunov-based flow solver," Advances in Water Resources, Vol. 68, pp. 42–61, 2014. DOI: 10.1016/j.advwatres.2014.02.013.

[14] I. Marina, H. Oana, "The Use of Hec-Ras Modelling in Flood Risk Analysis," Air & Water Components of the Environment/Aerul Si Apa Componente Ale Mediului, pp. 315-322, 2015.

[15] G. Papaioannou, L. Vasiliades, A. Loukas, A. Alamanos, A. Efstratiadis, A. Koukouvinos, I. Tsoukalas, P. Kossieris, "A flood inundation modeling approach for urban and rural areas in lake and large-scale river basins," Water, Vol. 13, No. 9, p. 1264, 2021. DOI: 10.3390/w13091264.

[16] P. Costabile, C. Costanzo, D. Ferraro, F. Macchione, G. Petaccia, "Performances of the new HEC-RAS version 5 for 2-D hydrodynamic-based rainfall-runoff simulations at basin scale: Comparison with a state-of-the art model," Water, Vol. 12, No. 9, p. 2326, 2020. DOI: 10.3390/W12092326.

[17] H. El-Bagoury, A. Gad, "Integrated Hydrological Modeling for Watershed Analysis, Flood Prediction, and Mitigation Using Meteorological and Morphometric Data, SCS-CN, HEC-HMS/RAS, and QGIS," Water, Vol. 16, No. 2, p. 356, 2024. DOI: 10.3390/w16020356.

[18] N. N. Zainal, S. H. A. Talib, "Review paper on applications of the HEC-RAS model for flooding, agriculture, and water quality simulation," Water Practice and Technology, Vol. 19, No.7, pp. 2883-2900, 2024. DOI: 10.2166/wpt.2024.173.

[19] G. W. Brunner, "Benchmarking of the HEC-RAS Two-Dimensional Hydraulic Modeling Capabilities," U.S Army Corps of Engineers: Institute for Water Resources, pp. 1–137, 2018.

[20] P. Costabile, C. Costanzo, D. Ferraro, P. Barca, "Is HEC-RAS 2D accurate enough for storm-event hazard assessment? Lessons learnt from a benchmarking study based on rain-on-grid modelling," Journal of Hydrology, Vol. 603, 2021. DOI: 10.1016/j.jhydrol.2021.126962.

[21] I. Shustikova, A. Domeneghetti, J. C. Neal, P. Bates, A. Castellarin, "Comparing 2D capabilities of HEC-RAS and LISFLOOD-FP on complex topography," Hydrological Sciences Journal, Vol. 64, No. 14, pp. 1769–1782, 2019. DOI: 10.1080/02626667.2019.1671982.

[22] M. A. Bragg, A. Poudel, J. G. Vasconcelos, "Comparing SWMM and HEC-RAS Hydrological Modeling Performance in Semi-Urbanized Watershed," Water, Vol. 17, No. 9, p. 1331, 2025. DOI: 10.3390/w17091331.

[23] M. Patel, F. Parekh, "Advanced Techniques of Flood Forecasting, Flood Inundation Mapping and Flood Prioritization of Panam River Basin," Civil Engineering and Architecture, Vol. 10, No. 4, pp. 1303–1316, 2022. DOI: 10.13189/cea.2022.100406.

[24] V. M. Quirogaa, S. Kurea, K. Udoa, A. Manoa, "Application of 2D numerical simulation for the analysis of the February 2014 Bolivian Amazonia flood: Application of the new HEC-RAS version 5," Ribagua, Vol. 3, No. 1, pp. 25–33, 2016. DOI: 10.1016/j.riba.2015.12.001.

[25] A. A. Shaikh, A. I. Pathan, S. I. Waikhom, P. G. Agnihotri, M. N. Islam, S. K. Singh, "Application of latest HEC-RAS version 6 for 2D hydrodynamic modeling through GIS framework: a case study from coastal urban floodplain in India," Modeling Earth Systems and Environment, Vol. 9, No. 1, pp. 1369–1385, 2023. DOI: 10.1007/s40808-022-01567-4.

[26] E. Yalcin, "Assessing the impact of topography and land

cover data resolutions on two-dimensional HEC-RAS hydrodynamic model simulations for urban flood hazard analysis," Natural Hazards, Vol. 101, No. 3, pp. 995–1017, 2020. DOI: 10.1007/s11069-020-03906-z.

[27] J. L. Ayog, "Benchmarking the capabilities of the latest HEC-RAS version 6.3 in simulating varying flood flows," 16th Seminar on Science and Technology 2023, Faculty of Science & Natural Resources, Universiti Malaysia Sabah, Sep. 2023.

[28] M. Paudel, S. B. Roman, J. Prichard, "A Comparative Study of HEC-RAS 2D, Tuflow, & Mike21," ASFPM 2016 Annual National Conference, Grand Rapids, Michigan, 2016.

[29] P. Artiglieri, G. Curulli, F. Coscarella, D. Algieri Ferraro, F. Macchione, "Performance of HEC-RAS v6.5 at basin scale for calculating the flow hydrograph: comparison with TUFLOW," Natural Hazards, Vol. 121, No. 8, pp. 9477-9490, 2025. DOI: 10.1007/s11069-025-07170-x.

[30] T. Molls, G. Brunner, A. Sanchez, "Comparing HEC-RAS v5.0 2-D Results with Verification Datasets," Sacramento FMA conference, U.S Army Corps of Engineers: Institute for Water Resources, 2016.

[31] US Army Corps of Engineers. HEC-RAS Hydraulic Reference Manual Version 6.6, 2024.

[32] R. Sabeti, I. Stamataki, T. R. Kjeldsen, "Reconstructing the 1968 River Chew flash flood: merging a HEC-RAS 2D hydraulic modelling approach with historical evidence," Geomatics, Natural Hazards and Risk, Vol. 15, No. 1, 2024, DOI: 10.1080/19475705.2024.2377655.

[33] A. P. Sharma, X. Fu, G. R. Kattel, T. R. Adhikari, M. A. Hassan, "Appraising flood risk and inundation extent using GIS-aided 2D hydraulic modeling in Nepal Himalaya: A case of West Rapti River Basin," Modeling Earth Systems and Environment, Vol. 11, No. 3, 2025, DOI: 10.1007/s40808-025-02356-5.

[34] T. Namgyal, D. A. Thakur, R. D.S, M. P. Mohanty, "Are open-source hydrodynamic models efficient in quantifying flood risks over mountainous terrains? An exhaustive analysis over the Hindu-Kush-Himalayan region," Science of the Total Environment, Vol. 897, p. 165357, 2023, DOI: 10.1016/j.scitotenv.2023.165357.

[35] G. A. M. De Almeida, P. Bates, "Applicability of the local inertial approximation of the shallow water equations to flood modeling," Water Resources Research, Vol. 49, No. 8, pp. 4833–4844, 2013, DOI: 10.1002/wrcr.20366.

[36] S. Dazzi, R. Vacondio, A. Dal Palù, P. Mignosa, "A local time stepping algorithm for GPU-accelerated 2D shallow water models," Advances in Water Resources, Vol. 111, pp. 274–288, 2018, DOI: 10.1016/j.advwatres.2017.11.023.

[37] P. Hu, Y. Lei, J. Han, Z. Cao, H. Liu, Z. He, Z. Yue, "Improved Local Time Step for 2D Shallow-Water Modeling Based on Unstructured Grids," Journal of Hydraulic Engineering, Vol. 145, No. 12, p. 06019017, 2019, DOI: 10.1061/(ASCE)HY.1943-7900.0001642.

[38] B. F. Sanders, "Integration of a shallow water model with a local time step," Journal of Hydraulic Research, Vol. 46, No. 4, pp. 466–475, 2008, DOI: 10.3826/jhr.2008.3243.

[39] K. Sharir, R. Roslee, "Analysis of Physical, Social and Environmental Flood Vulnerability Index in Kota Belud Area, Sabah, Malaysia," Sains Malaysiana, Vol. 52, No. 6, pp. 1619–1633, 2023. DOI: 10.17576/jsm-2023-5206-02.

[40] L. T. Chai, A. Nainar, R. Roslee, W. V. C. Wong, M. H. Phua, "Assessment of immediate and five-year earthquake impacts on river systems in Sabah, Malaysia using multi-temporal satellite imageries," Geoenvironmental Disasters, Vol. 11, No. 1, p. 16, 2024. DOI: 10.1186/s40677-024-00276-7.

[41] A. Jafar, R. Dollah, N. Sakke, M.T. Mapa, E.P. Joko, M.M. Radzi, U. Imang, S.A. Ahmad, A. Ab. Wahab, J.A. Sipatau, "Tourism and Natural Hazards: River Landform Changes Due to Geohazards and Its Influence on the Economic Development of Ecotourism in Sabah, Malaysia," Sustainability, Vol. 14, No. 23, p. 15832, 2022. DOI: 10.3390/su142315832.

[42] Online Available: https://www.theborneopost.com/2021/05/08/melangkap-eco-tourism-products-get-boost-from-sabah-new-deal/

[43] K. Sharir, G. T. Lai, N. Simon, L. K. Ern, E. Madran, R. Roslee, "Debris flow susceptibility analysis using a bivariate statistical analysis in the Panataran River, Kg Melangkap, Sabah, Malaysia," IOP Conference Series: Earth and Environmental Science, Vol. 1103, p. 012038, 2022. DOI: 10.1088/1755-1315/1103/1/012038.

[44] R. Ramli, J. L. Ayog, M. F. T. Ngui, R. Roslee, F. Tongkul, M. R. Taharin, "Braiding Intensity Analysis of a Post-Seismic Debris Flow Event Using a Comprehensive Indexing Tool," Environment and Ecology Research, Vol. 13, No. 2, pp. 241–250, 2025. DOI: 10.13189/eer.2025.130205.

[45] O. G. Salawu, D. Leke, "Assessment of Changes in Channel Width and Braiding: The Implications on Flooding Upstream of Shiroro Reservoir in river Kaduna, Kaduna State, Nigeria," Journal of Applied Sciences and Environmental Management, Vol. 28, No. 1, pp. 179–186, 2024, DOI: 10.4314/jasem.v28i1.20.

[46] Online Available: https://www.theborneopost.com/2022/12/23/firefighters-rescue-25-trapped-by-flooding-at-kota-belud-campsite/